

# Application of CFD in Nanoremediation Problems with Nanoscale Zero-Valent Iron Particles

Amanda B. de Almeida<sup>a,\*</sup>, Eliton Fontana<sup>a</sup>, Alex V. L. Machado<sup>b</sup>, Luiz F. L. Luz Jr.<sup>a</sup>

<sup>a</sup> Chemical Engineering Department, Federal University of Paraná, Curitiba, PO Box 19011, 81531-980, Brazil

<sup>b</sup> Chemical Engineering Program, Federal University of Rio de Janeiro, Rio de Janeiro, PO Box 68502, 21941-972, Brasil  
 amandaborges.almeida@gmail.com

TCE (Trichloroethylene) is a chlorinated solvent, known for its toxicity present in many underground water reservoirs and, as it is a less viscous and denser contaminant than water, it reaches the impermeable substrate of the reservoirs, remaining trapped in the water system pores for years or decades. The TCE removal technique studied in this work is the reduction by nanoparticles of zero valent iron. In this case, Fe<sup>0</sup> acts as an electron donor so that TCE is reduced to less harmful compounds that are easier to remove. And, just as important as the reduction of TCE through the chemical reaction, are the pressure disturbances caused by the injection of the solution of nanoparticles and by the gas that is one of the products of the reaction. These disorders can displace the TCE from the interior of the pores, facilitating its later removal. Through computational fluid dynamics simulations, using openFOAM free software, it was possible to prove that ethylene, which is one of the products of the TCE reduction reaction, is capable of displacing DNAPL from the interior of the pores. Through two-dimensional simulations, a 97% reduction in TCE saturation was obtained due to displacement of the contaminant out of the field of view. It is also worth noting that the simulations performed were consistent with experimental results performed by other authors. In addition, the behaviour of the TCE - water flow was also evaluated as a function of the contact angle TCE - water - grain wall. In this case, there was a greater recovery of the TCE for its drainage condition, with contact angles of approximately 140°.

## 1. Introduction

Trichloroethylene (TCE) is a non-flammable, volatile, colourless, slightly sweet-smelling chlorinated solvent belonging to the most abundant and common class of contaminants, chlorinated volatile organic compounds (VOCs), which pose a risk to human health and ecosystems. due to its known toxicity. TCE was first detected in the United States in 1977 and has since been one of the most common contaminants in groundwater (Tabrez, 2009). The maximum contaminant level is 10 mg/L for trichloroethylene in the European Union and is lower for groundwater in some countries (Pak et.al., 2020). The need for alternative DNAPL remediation methods leads to the development of new technologies, such as soil washing, chemical oxidation, bioremediation, reactive barriers, and nanoremediation (Pak et.al., 2019).

The rates and pathways of the TCE reduction by zero-valent iron filings have been intensively studied and are well known. TCE is reduced and releases chloride ions, while iron is oxidized and supplies electrons. The oxidation mechanisms proposed by LIU, et.al. (2005) are  $\beta$ -elimination (mainly), hydrogenolysis and hydrogenation (the last two are less expressive). These mechanisms explain the formation of ethylene and ethane as main products (Liu et al., 2005).

Nanoremediation employs nanoscale iron particles (nZVI) that are extremely reactive and excellent electron donors (Pak et.al., 2019). Many studies report the degradation of NAPLs using iron particles, but the great advantage of using nanoparticles is the increase in the surface area and, therefore, an increase in the speed of the degradation reaction. Pak, et al. (2020) showed how the TCE degradation reaction with nanoscale zero-valent iron particles (nZVI) occurs in a condition similar to that which occurs in an aquifer, that is, what happens in the rock pores during this interaction between nanoparticles and contaminants. The main objective of this work was to show the redistribution of TCE inside the pores due to the formation of the gas (product of the

chemical reaction that occurs in the TCE/nZVI interface) and, with that, to obtain a favorable redistribution to reduce the saturation of the contaminants that are trapped inside aquifer pores. For this, 4D experiments (time - resolved three dimensions) were carried out using the X-ray microtomography (IMX) beamline at the Brazilian Synchrotron Light Laboratory (LNLS/CNPEM) using a bed of glass spheres of 250 to 500  $\mu\text{m}$  which represented medium and coarse sand with an estimated absolute permeability of  $1.7 \times 10^{-11} \text{ m}^2$  (internal diameter = 2.5 mm, length = 33 mm and porosity of 38%). Within the imaged section of the sample TCE showed an approximate 57% reduction in saturation because of gas-induced remobilization (Pak et.al., 2020).

Many studies are published to understand and improve the mobility of the suspension of iron nanoparticles in porous media, but it is important to evaluate the dynamics of the two-phase reactive flow as a whole. This work aims to evaluate the behaviour of all components present inside the pore system during the treatment process of aquifers contaminated with TCE through CFD simulations using openFOAM, which has the great advantage of being license free and presenting open code. In this way, it is possible to advance to the field treatment stage with greater assertiveness, saving resources and time in the remediation process. Another goal of this paper is the performance of CFD simulations using microtomography images in order to evaluate the dynamics of the TCE and the gases that can be generated by the chemical reaction inside the pores. Such simulations are of great importance due to the great difficulty of carrying out experiments using TCE, as it is extremely toxic, and all disposals must be done with complete safety.

## 2. Materials and Methods

In the pre-processing stage are defined the mathematical model of the physical problem, the geometric model, the discretization of the geometric model (mesh), the numerical method that will be used for the discretization of the differential equations, the solution algorithm and the criteria for convergence. Regarding the geometric model, the simulation will be performed considering an orthogonal view of a bed of glass beads that represents the porous medium of a groundwater system. Pak et. al, 2020 made available the images obtained by X-ray microtomography in their experiments. These images are formed by 624 slices that form a representation in three dimensions of  $1,024 \times 1,024 \times 624$  voxels ( $3.36 \times 3.36 \times 2.05 \text{ mm}^3$ ). The initial water injection flow rate ranged from 100 to 1,000  $\mu\text{L}/\text{min}$  on the lower face of the bed (Bottom face).

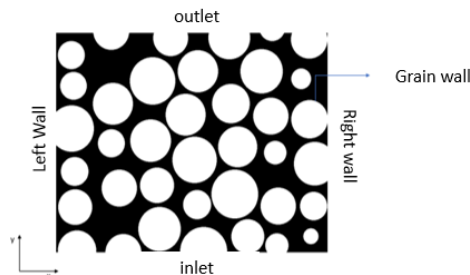


Figure 1. Binarized image

For the mesh generation, the algorithm developed by RAEINI et. al, 2012 voxelToFoam, was used, which was written in C++ language to be applied in OpenFOAM.

## 3. Mathematical model of the two-phase problem

In the case of isothermal flows of two immiscible fluids, the physical quantities analyzed are mass and moment. The biggest challenge of multiphase flows is in the treatment of the interface, that is, in capturing the place where the discontinuities of properties and stresses occur. The Volume of Fluid (VOF) model, which will be used in this work through the interFOAM solver, is an adaptation of the Euler-Euler two-fluid model and was proposed in 1981 by Hirt and Nichols (Prosperetti, 2009). A solver that implements the VOF technique for two immiscible, isothermal and incompressible fluids is employed. This means that the material properties are constant in the region filled by one of the two fluids, except at the interface. Therefore, the continuity and momentum equations must be solved for both fluids together with the transport equation of the alpha fluid fraction ( $\alpha$ ) (Cano-Lozano, 2014):

$$\nabla \mathbf{u} = 0 \quad (1)$$

$$\frac{\partial \rho \mathbf{u}}{\partial t} + \nabla \cdot (\rho \mathbf{u} \mathbf{u}) = -\nabla p + \nabla \boldsymbol{\tau} + \rho \mathbf{g} + \sigma \kappa \nabla \alpha \quad (2)$$

$$\frac{\partial \alpha}{\partial t} + \nabla \cdot (\mathbf{u}\alpha) = 0 \quad (3)$$

### 3.1 Numerical implementation in OpenFOAM

In equations 1, 2 and 3  $\mathbf{u}$  is the velocity field defined as a weighted velocity, based on the volume fraction distribution:

$$\mathbf{u} = \mathbf{u}_1\alpha + \mathbf{u}_2(1 - \alpha) \quad (4)$$

$\mathbf{u}_1$  denotes the velocity of the fluid 1,  $\mathbf{u}_2$  the velocity of the fluid 2 and  $\boldsymbol{\tau}$  represents the viscous stress tensor:

$$\boldsymbol{\tau} = \mu[\nabla\mathbf{u} + (\nabla\mathbf{u})^T] \quad (5)$$

$\sigma$  is the surface tension, considered constant;  $\mathbf{g}$  represents the acceleration of gravity and  $\kappa$  is the average curvature of the interface:

$$\kappa = \nabla \cdot \left( \frac{\nabla\alpha}{|\nabla\alpha|} \right) \quad (6)$$

The calculation of the local properties where the interface is present is based on the average of the properties of both fluids weighted by the scalar field  $\alpha$  (Cano-Lozano, 2014):

$$\rho_i = \alpha\rho_1 + (1 - \alpha)\rho_2 \quad (7)$$

$$\mu_i = \alpha\mu_1 + (1 - \alpha)\mu_2 \quad (8)$$

In interFOAM, the algorithm for solving the scalar transport  $\alpha$  is known as MULES (Multi-Dimensional Limiter for Explicit Solution). In this case, it adds an artificial compression term to the transport equation of  $\alpha$  so that the interface is as dispersed as possible, resulting in:

$$\frac{\partial \alpha}{\partial t} + \nabla \cdot (\mathbf{u}\alpha) + \nabla \cdot [u_c\alpha(1 - \alpha)] = 0 \quad (9)$$

Where the compressibility term  $u_c$  acts only in the interfacial region. Also called compression speed, this term is defined as follows:

$$u_c = \min[C_\alpha|\mathbf{u}|, \max(|\mathbf{u}|)] \frac{\nabla\alpha}{|\nabla\alpha|} \quad (10)$$

The boundary conditions are defined in the time directory 0. In two-phase simulations, the constant volumetric flow was considered equal to 10  $\mu\text{L}/\text{min}$  entering in the positive direction of the y-axis on the Bottom face. Consequently, the material output was defined by the Top face. The initial internal field (`internalField`) in each control volume is considered uniform and equal to zero, that is, the initial velocity field is stagnant.

As it is a two-phase simulation, it is necessary to define the initial volumetric fraction ( $\alpha$ ) of one of the components. Therefore, in the time directory 0 the `alpha.TCE` file is defined.

The simulations start with water in the entire domain, so the `internalField` is uniform equal to zero and between the time instants 0 and 20ms it adds pure TCE. After 20ms pure water is fed again. In this case, the volumetric fraction of the TCE is varied, which at time 0 is null, between 0 and 20ms it is equal to 1 and after 20ms it becomes null again.

## 4. Results and discussion

As the objective is to understand the dynamics of the flow of TCE and water in porous media under different wettability conditions, the invading fluid (water) is considered injected into the porous medium saturated with the defending fluid (TCE) with a constant flow rate of  $10^{-6}$  L/min. The defending fluid is what is intended to be recovered and the invading fluid is what will be injected into the pore system to displace the defending fluid. The contact angle is defined as a function of the densest fluid, which in this case is the TCE. In these simulations, it starts with water throughout the domain, then TCE (defense fluid) is added and after 20ms water is added again (invading fluid). Four simulations were performed evaluating different scenarios of contact angles.

In the next images it is possible to observe the TCE saturation in time instant 0.089 seconds for different contact angles:

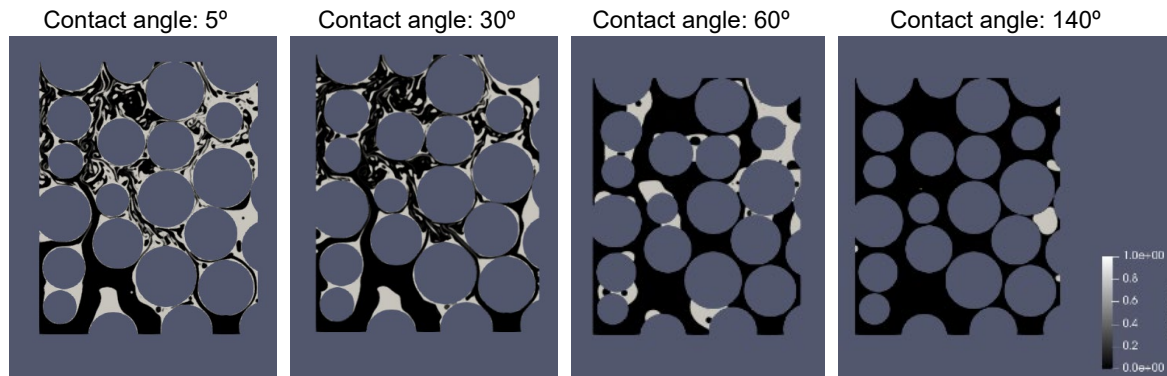


Figure 2: TCE saturation in time instant 0.089 seconds for different contact angles

Comparing the images obtained at the end of the simulation, it is possible to observe that the TCE is more easily drained in the condition of greater contact angle. In Figure 2 the volume is almost all occupied by water, indicating that most of the TCE has left the field of view. As the contact angle increases, the TCE becomes less wetting, so it does not even enter the smaller pores, making it easier to drain. Newell et al. emphasize in their work that the wetting fluid is the one that has the property of covering solid surfaces and occupying the smallest pores of the soil and the non-wetting fluid, in turn, is restricted to occupying the largest pores.

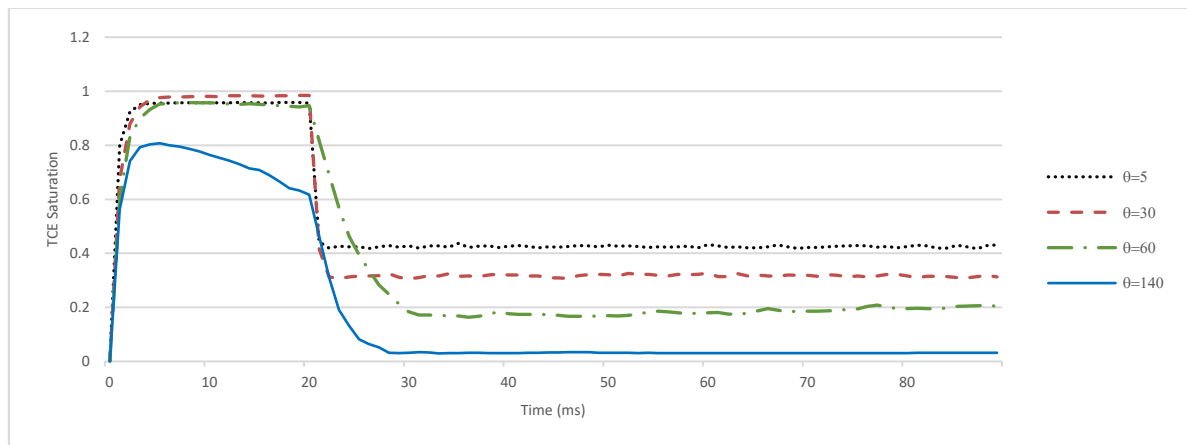


Figure 3: TCE saturation as a function of contact angle

Evaluating Figure 3, it is observed that in the case of a contact angle of  $140^\circ$ , the saturation of the TCE does not reach unity, as in the case of smaller contact angles, indicating once again that, as it is a drainage condition, the wetting fluid is water, so the TCE preferentially occupies the larger pores. As TCE is denser than water, for contact angles greater than  $90^\circ$  the water wets the solid more and a situation of drainage of the denser fluid (TCE) is observed. It is important to highlight the influence of density and viscosity on defending fluid recovery. In this case, the defending fluid (TCE) is the densest, so the contact angle is defined for the TCE. Thus, a contact angle of  $140^\circ$  indicates low wettability of the defending fluid, therefore a greater recovery of the same, since from the beginning of the simulation its occupation is restricted to the largest pores. Comparing the simulations with different values of contact angle, it is observed that the situation of drainage of the defense fluid (TCE) is reached for an angle of  $140^\circ$  (low wettability of the defending fluid), given that after the injection of water in the time after 20ms the TCE saturation drops to values below 5%. In this case, the invading fluid (water) presents greater wettability and the TCE, by presenting lower wettability, did not even enter the smallest pores. For the case of strong wettability of the defense fluid (TCE), it enters the smaller pores, as it is the most wetting fluid, being retained in the porous medium and at the end of the simulation ( $t=89\text{ms}$ ) its saturation is still 43%.

To evaluate the TCE flow in the pore system in the presence of a gas phase, a simulation was performed using the *multiphaseInterFoam* solver, which is based on the Fluid Volume (VOF) method. In this simulation, the volume starts saturated with water, TCE is fed into the Bottom face, at 100ms it feeds water again into the Bottom face and at 130ms it feeds ethylene into the same face. The objective is to verify if the gas (which would be one of the products of the TCE reduction reaction), helps to remove TCE from the interior of the pores. The simulation was performed considering the contact angle of  $90^\circ$  (which is the default contact angle used in openFOAM). The ethylene feed that will be defined in OpenFOAM is calculated based on the chemical reaction

kinetics and reaction stoichiometry. The ethylene feed rate is determined from the kinetics of the chemical reaction proposed by (Liu et al., 2005).

$$\frac{dC_{TCE}}{dt} = -k_{SA} \cdot a_s \cdot \rho_m \cdot C_{TCE} \quad (11)$$

The use of RNIP-type nanoparticles and excess TCE are considered, therefore, according to TABLE 1, the chemical reaction and the specific kinetic constant of the reaction is:

Table 1: Chemical reaction and kinetic constant considered in this simulation.

Excess TCE	Kinetic Constant (L h <sup>-1</sup> m <sup>-2</sup> )
$CHCl_3 + 3Fe^0 + H^+ \rightarrow C_2H_2 + 3Fe^{2+} + 3Cl^-$	$k_{SA} = 3.3 \pm 0.06 \times 10^{-4}$

The specific area of RNIP nanoparticles ( $a_s$ ) is 23 m<sup>2</sup>g<sup>-1</sup> and the iron concentration ( $\rho_m$ ) is 0.36 gL<sup>-1</sup> (Liu et al., 2005). Integrating equation (11) we obtain the relationship between the concentration of TCE as a function of reaction time, where  $C_{TCE,0}$  is the initial TCE saturation equal to 7%. This value was obtained through the simulation, considering only the water flow to reduce the TCE, that is, it is the saturation of the TCE just before starting the ethylene feed. In the experiments by Liu et. al TCE is no longer consumed after 6 days (144 hours) of experiment, so this reaction time is considered. The result is the saturation of the TCE after 6 days of reaction:

$$\%_{TCE} = 0.07 \cdot e^{(-3.3 \times 10^{-4} \times 23 \times 0.36) \times 144} = 0,047 \quad (12)$$

That is, at the end of the reaction, 0.047g of TCE per 100g of solution remains in the medium, which represents a consumption of 0.023g of TCE per 100g of solution. ( $1.75 \times 10^{-4}$  mol of TCE per 100g of solution). The rate of ethylene formation is obtained through the stoichiometry of the reaction. It is observed that 1 mol of TCE produces 1 mol of ethylene.  $1.75 \times 10^{-4}$  mol of ethylene, in 100g of solution in a time of 144 hours, represents a mass flow rate of  $9,47 \times 10^{-11} \frac{kg}{s}$  (considered in the simulations as ethylene feed).

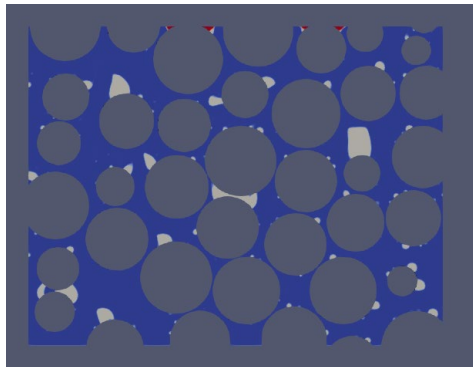


Figure 4: Simulation in the instant of time 130ms, before starting the feeding of ethylene on the bottom face

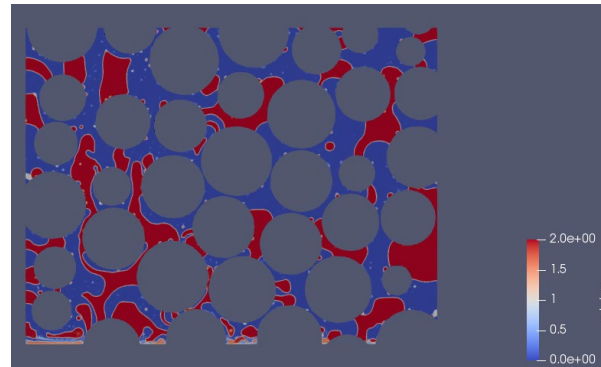


Figure 5: Simulation in the instant of time 200ms, after the feeding of ethylene on the bottom face

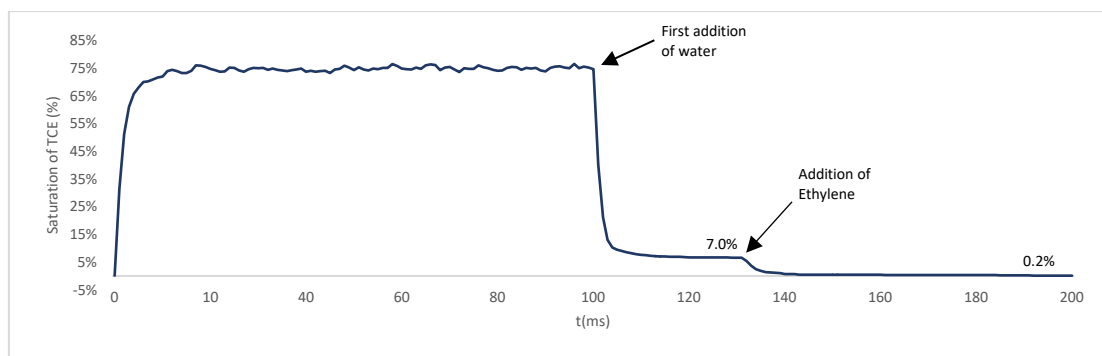


Figure 6: Variation of the saturation over time

Through the images obtained through PARAVIEW™ (Figures 4 and 5), it is possible to verify that there was a displacement of the TCE from the interior of the pores to outside the field of view. Therefore, to prove the visual results of the images, an analysis of the saturation of the TCE was carried out over time. The graph is shown in Figure 6. It is observed that after the ethylene supply, the TCE saturation drops from approximately 7.0% to 0.2%, which represents a decrease of 97%, indicating that the gas is really capable of displacing the contaminant out of the pores in which it is trapped. The fluctuation observed before the addition of water is normal due to TCE entering and leaving the control volume (this is a physical fluctuation, not a numerical one).

## 5. Conclusions

It was possible to create the 2D mesh from the binarized microtomography images and perform the multiphase simulation to evaluate the behavior of fluids (TCE – water – ethylene) in the pore system. Evaluating the flow in different conditions of contact angle, it was possible to observe that the highest percentage of TCE recovery is obtained in conditions of drainage of the same, with high values of contact angle. It was also observed that ethylene, one of the products of the TCE reduction reaction in aqueous medium with zero valent iron nanoparticles, contributes to its redistribution, with this it is possible to obtain a reduction in the saturation of DNAPL contaminants that are trapped in the inside the pores. Through the simulation, after the addition of ethylene at a rate simulating the one that would be obtained through the chemical reaction, a reduction of 97% of the TCE that was in the field of view was obtained and the final saturation of the contaminant was 0.002 %. This result is more positive than that obtained in the experiments by Pak, et al (2020), who obtained a final TCE saturation of 2.34% after 387 minutes of experiment. In this case, it is important to note that simulations were performed in only 2 dimensions.

## References

- Hirt C. W., Nichols B. D., 1981, Volume of fluid (VOF) method for the dynamics of free boundaries. *Journal of Computational Physics*, 39, 201–225. <doi.org/10.1016/0021-9991(81)90145-5>
- Liu Y., Majetich S. A., Tilton R. D., Sholl D. S., Lowry G. V., 2005, TCE dechlorination rates, pathways, and efficiency of nanoscale iron particles with different properties. *Environmental Science and Technology*, 39, 1338–1345. <doi.org/10.1021/es049195r>
- Newell C. J., Acree D. A., Randall R. R., Huling S. G., 1995, Light Nonaqueous Phase Liquids. *Ground Water Issue*, 1–28.
- Pak T., Archilha N. L., Lima Luz L. F., 2019, *Nanotechnology Characterization Tools for Environment, Health, and Safety*. 1<sup>st</sup> ed. Springer, Cambridge, MA, USA.
- Pak T., Lima Luz L. F., Tosco, T., 2020, Pore-scale investigation of the use of reactive nanoparticles for in situ remediation of contaminated groundwater source. *Proceedings of the National Academy of Sciences of the United States of America*, 117, 13366–13373. <doi.org/10.1073/pnas.1918683117>
- Prosperetti A., Tryggvason G., 2009, *Computational Methods for Multiphase Flow*. Cambridge University Press, 2009
- Raeini A. Q., Blunt M. J., Bijeljic B., 2012, Modelling two-phase flow in porous media at the pore scale using the volume-of-fluid method. *Journal of Computational Physics*, 231, 5653–5668. <dx.doi.org/10.1016/j.jcp.2012.04.011>
- Scardovelli R., Zaleski S., 1999, Direct numerical simulation of free-surface and interfacial flow. *Annual Review of Fluid Mechanics*, 31, 567–603. <doi.org/10.1146/annurev.fluid.31.1.567>
- Tabrez S., Ahmad M., 2009, Toxicity, biomarkers, genotoxicity, and carcinogenicity of trichloroethylene and its metabolites: A review. *Journal of Environmental Science and Health - Part C Environmental Carcinogenesis and Ecotoxicology Reviews*, 27, 178–196. <doi.org/10.1080/10590500903091340>
- Tosco T., Petrangeli P., M., Cruz V. C., Sethi R., 2014, Nanoscale zerovalent iron particles for groundwater remediation: A review. *Journal of Cleaner Production*, 77, 10–21. <dx.doi.org/10.1016/j.jclepro.2013.12.026>